



In silico prediction of human carboxylesterase-1 (hCES1) metabolism combining docking analyses and MD simulations

Giulio Vistoli ^{a,*}, Alessandro Pedretti ^a, Angelica Mazzolari ^a, Bernard Testa ^b

^a Dipartimento di Scienze Farmaceutiche 'Pietro Pratesi', Facoltà di Farmacia, Università degli Studi di Milano, Via Mangiagalli, 25, I-20133 Milano, Italy

^b Department of Pharmacy, University Hospital Centre (CHUV), Rue du Bugnon, CH-1011 Lausanne, Switzerland

ARTICLE INFO

Article history:

Received 14 August 2009

Revised 26 October 2009

Accepted 27 October 2009

Available online 31 October 2009

Keywords:

Esterases

Human carboxylesterase-1

Metabolism prediction

Docking analysis

Molecular dynamics

ABSTRACT

Metabolic problems lead to numerous failures during clinical trials, and much effort is now devoted in developing in silico models predicting metabolic stability and metabolites. Such models are well known for cytochromes P450 and some transferases, whereas little has been done to predict the hydrolytic activity of human hydrolases. The present study was undertaken to develop a computational approach able to predict the hydrolysis of novel esters by human carboxylesterase hCES1. The study involves both docking analyses of known substrates to develop predictive models, and molecular dynamics (MD) simulations to reveal the *in situ* behavior of substrates and products, with particular attention being paid to the influence of their ionization state. The results emphasize some crucial properties of the hCES1 catalytic cavity, confirming that as a trend with several exceptions, hCES1 prefers substrates with relatively smaller and somewhat polar alkyl/aryl groups and larger hydrophobic acyl moieties. The docking results underline the usefulness of the hydrophobic interaction score proposed here, which allows a robust prediction of hCES1 catalysis, while the MD simulations show the different behavior of substrates and products in the enzyme cavity, suggesting in particular that basic substrates interact with the enzyme in their unprotonated form.

© 2009 Elsevier Ltd. All rights reserved.

1. Introduction

More than half of drug candidates fail during clinical trials due to an unsuitable pharmacokinetic profile. For this reasons, the most recent strategies in drug discovery and development give attention to an ADMET profiling of new molecules with the clear aim to select (and develop) only drug-like compounds with an optimal pharmacokinetic profile. Such an early pharmacokinetic analysis requires the assessment of a maximum of useful and relevant molecular properties that allow a reliable prediction of drug-likeness also for large molecular libraries.¹

As a result, much research effort has been invested in developing in silico tools to predict physicochemical properties relevant to pharmacokinetic profile, for example, aqueous solubility and lipophilicity. Similarly, predictive tools for metabolic stability are clearly useful since inadequate metabolism represents one of the most problematic failures during clinical trials. For metabolism, however, global quantitative approaches predictive of heterogeneous molecular datasets are virtually impossible, given the large arsenal of diverse and not fully investigated enzymes involved in human xenobiotic metabolism. And indeed, most computational

approaches in the recent literature are restricted to specific metabolizing enzymes.^{2,3}

The metabolizing activity of the most relevant red-ox enzymes⁴ (i.e., cytochromes P450,⁵ monoamine oxidases,⁶ and alcohol dehydrogenases⁷) and those of some significant conjugating enzymes⁸ (e.g., UDP-glucuronosyltransferases,⁹ sulfotransferases,¹⁰ methyltransferases,¹¹ and glutathione-S-transferases¹²) have been investigated in great detail by computational techniques and can be successfully predicted by several approaches. Conversely, little has been done to rationalize and predict *in silico* the hydrolyzing activity of the human hydrolases,¹³ although they play key roles in the hydrolytic metabolism of xenobiotics as well as in the activation of most prodrugs.¹⁴

Prodrug strategies^{15,16} allow, for example, the protection of some critical function in active agents and yield compounds with, for example, increased solubility, better bioavailability, or targeted active absorption. Clearly, such prodrugs must be promptly transformed into the active agent, a reaction that in most cases is one of hydrolysis. Thus, the possibility to predict the likelihood of a prodrug being efficiently transformed into the corresponding active form becomes of crucial importance when designing optimal prodrugs.

Carboxylesterases^{17,18} play a pivotal role in the hydrolysis of a variety of drugs or prodrugs featuring an ester, amide or carbamate function. Mammalian carboxylesterases (CESs) are members of the

* Corresponding author.

E-mail address: giulio.vistoli@unimi.it (G. Vistoli).

serine hydrolase family (also termed α/β -hydrolases).¹⁹ It has been suggested that CES isozymes can be classified into five proteins denominated CES1–CES5 according to their sequence homology. The majority of CESs so far identified belongs to the CES1 or CES2 families. CESs show ubiquitous tissue expression profiles in many mammalian species, with the highest levels in liver microsomes.²⁰

The experimental structures available for CES1 showed that the enzyme can be divided in three functional domains. The catalytic domain contains the active site with the catalytic triad. The $\alpha\beta$ domain stabilizes the trimeric architecture and assists the product release. Finally, the regulatory domain (also called Z-site) influences the trimer–hexamer equilibrium and modulates the binding site accessibility. The substrate specificities of CES1 and CES2 are considered as significantly different. CES1 mainly hydrolyzes substrates with a smaller alkyl/aryl group and a larger acyl group, although its wide catalytic pocket also allows structurally diverse compounds with a large alkyl/aryl moiety to be recognized. In contrast, the CES2 enzyme recognizes substrates with larger alkyl/aryl groups and smaller acyl groups, and its specificity may be constrained by structural hindrance in the active pocket.²¹

This study was undertaken to develop a computational approach able to successfully predict and rationalize the hydrolytic metabolism of novel esters by the human CES1 enzyme (hCES1, also termed hCES1A1). Since several X-ray structures have been resolved for the hCES1 enzyme (as deposited in the PDB database), our docking analyses involved a number of experimental structures suitably chosen to account for structural flexibility of the catalytic site. The study was subdivided into three parts: (a) choice and refinement of the most suitable X-ray experimental structures of the enzyme; (b) docking analyses of known substrates to develop robust predictive models also incorporating new scoring functions designed to take hydrophobic interactions into account; and (c) molecular dynamics (MD) simulations of some complexes to verify their stability and the influence of the ionization state of substrates and products.

2. Results

2.1. Choice of optimal CES1 structures for docking

The first step in our study was choosing the optimal hCES1 structures to be used in the docking analyses. Such simulations involved more resolved structures, since, as recently reviewed by Totrov and Abagyan,²² a collection of resolved structures bound to a variety of ligand classes can offer an ensemble of conformations which overcomes the static nature of crystal structures and can elucidate the structural changes that may occur upon ligand binding. As detailed below, the available experimental structures were compared and attention was focused on the most diverse

structures which reasonably represent different conformational states of the enzyme.

Until now, 13 experimental structures for human CES1 have been deposited in the PDB Database. Since the enzyme in the *apo* state has not been resolved yet, all published X-ray structures of the enzyme are complexes with an inhibitor, a substrate analogue or a product. Complexes with non-competitive inhibitors (e.g., tamoxifen and tacrine) were discarded since their binding sites are distant from the catalytic site and may distort the binding cavity into unphysiological conformations. Similarly, the structures of hCES1 covalently bound to inhibitors were ignored.

Specifically, Table 1 reports the similarities between the nine remaining experimental hCES1 structures as obtained by pair-wise rmsd values computed for the backbone atoms only. Clearly, the similarities between these structures are high, the main differences concerning the binding cavity. The greatest rmsd value (as evidenced in bold in Table 1) is seen between the complex with benzoate (PDB Id: 1YAJ), an enzymatic product resulting from the degradation of the inhibitor benzil (diphenylethane-1,2-dione) via a retro-alcohol condensation followed by hydrolysis,²³ and the complex with naloxone methiodide, an opiate antagonist (PDB Id: 1MX9).²⁴

When considering the small size of benzoate, a metabolite that cannot markedly distort the catalytic cavity during its egress, one can argue that the first CES1 structure should be similar to the enzyme in the *apo* state. In contrast, the complex with naloxone may represent the *holo* state since the enzyme accommodates a large substrate, meaning that its binding cavity should be large enough to encompass any other molecule of comparable size. The relevance of hCES1 in complex with naloxone is also due to the fact that, in contrast to typical substrates, this ligand has a large alkyl/aryl group and a small acyl group and this may significantly influence the architecture of the hCES1 catalytic site. As a consequence of this assumption, our docking analyses were based on these two experimental structures of hCES1, the one complexed with benzoate being termed *apo_CES1*, and the other complexed with naloxone being termed *holo_CES1*.

The binding pocket of the *apo_CES1* structure was gradually expanded by docking increasingly larger substrates (as explained under Methods), whereas the *holo_CES1* structure was exploited as determined experimentally because its catalytic pocket was wide enough to successfully accommodate all substrates considered here. The cavity expansion exerted on the *apo_CES1* structure does not alter the folding stability of the enzyme, as confirmed by (a) the limited increase in rmsd value between the two structures (the rmsd of the enlarged *apo_CES1* vs the *holo_CES1* was equal to 1.16 Å), (b) the very similar percentage of residues which fell in the allowed regions of a Ramachandran plot (76.3% in the enlarged *apo_CES1* vs 76.8% in the X-ray *apo_CES1*), and (c) the catalytic triad, which conserved its functional architecture in the enlarged

Table 1

Pair-wise comparison between the nine hCES1 experimental structures examined

PDB	Bound ligand	1YA8	1YAH	1YAJ	1MX5	1MX9	2DQY	2DQZ	2DR0
1YA8	Mevastatin (P)								
1YAH	Ethylacetate (P)	0.01							
1YAJ	Benzoate (P)	0.46	0.46						
1MX5	Homatropine (S)	0.29	0.29	0.55					
1MX9	Naloxone (S)	0.52	0.52	0.71	0.52				
2DQY	Cholate (P)	0.26	0.26	0.48	0.35	0.54			
2DQZ	Palmitate (P)	0.32	0.32	0.44	0.34	0.56	0.35		
2DR0	Taurocholate (P)	0.32	0.32	0.45	0.34	0.53	0.34	0.32	
2H7C	Coenzyme A (P)	0.45	0.45	0.52	0.46	0.62	0.41	0.44	0.46

Type of bound ligand: P = enzymatic product, S = substrate analogue.

The rmsd (root mean square deviation) values were computed considering the backbone atoms only and are expressed in Å. The greatest rmsd difference is evidenced in bold.

apo_CES1 structure. Indeed, in both structures (i.e., *apo_CES1* and *holo_CES1*) the polarity of Ser221 (which attacks the carbonyl group of the substrate) was enhanced by the closeness of the imidazole ring of His468 whose basicity was, in turn, increased by the neighboring Glu354. The Ser-His-Glu residues constitute the well-known catalytic triad which characterizes such superfamily of hydrolases and whose detailed mechanism can be found elsewhere.¹⁹

2.2. Docking results: prediction of CES1 activity

Four sets of docking simulations were carried out since the analyses involved two enzyme structures (i.e., *apo_CES1* and *holo_CES1*) each examining the substrates with basic groups in their unprotonated and protonated states (as also specified in Table 2A and B). Here, we first describe correlation studies aimed at identifying the best set of docking calculations and ultimately at focusing our analysis of docking results on the most predictive ones.

Table 3 reports the correlation equations (Eqs. 1–4) obtained for the training set of 25 substrates (Table 2A) in the four series of

docking simulations. All correlations included only three independent variables to guarantee their statistical robustness. The correlations reveal that (a) docking analyses performed using the *apo_CES1* structure (Eqs. 1 and 2) always afforded better correlations than those produced by the *holo_CES1* structure (Eqs. 3 and 4); and (b) in both cases the substrates with unprotonated basic groups (Eqs. 1 and 3) correlated better than the protonated ones (Eqs. 2 and 4) probably because the latter are biased by ionic contacts. This result may suggest that the neutral forms are probably better recognized by the enzyme than the cations.

Interestingly, the two relationships for unprotonated substrates include the same parameters. The same is true for their protonated forms. In other words, the factors that determine hCES1 recognition are strongly influenced by the ionization state of the basic groups irrespective of the apo or holo structure of the enzyme. All reported equations include the MLP_{Ins} parameter, confirming the crucial role of hydrophobic contacts in hCES1 binding. Although there is a fair and expected intercorrelation between MLP_{Ins} scores and virtual log *P* values as computed by the MLP

Table 2A
Substrates included in the training set

Substrate	Exp K_m (μM)	Exp pK_m	Pred pK_m	$\Delta(\text{exp} - \text{pred})$	Distance Ser221 (\AA)	MLP_{Ins}	Ref.
($\alpha R,1R$)- <i>cis</i> -A3	0.30	6.52	6.42	0.1	4.35	-2.35	29
($\alpha S,1R$)- <i>trans</i> -A3	0.70	6.15	5.65	0.5	4.13	-1.83	29
($\alpha S,1S$)- <i>cis</i> -A3	1.40	5.85	5.58	0.27	4.17	-1.80	29
($\alpha R,1S$)- <i>cis</i> -A3	1.50	5.82	5.34	0.48	4.30	-1.69	29
($\alpha R,1R$)- <i>trans</i> -A3	1.7	5.77	4.99	0.78	4.14	-1.44	29
($\alpha S,1S$)- <i>trans</i> -A3	2.40	5.62	5.61	0.01	4.71	-1.94	29
(<i>RS</i>)- <i>cis</i> -Permethrin	9.8	5.01	5.31	-0.3	5.63	-1.98	36
(<i>RR</i>)- <i>trans</i> -Permethrin	23.8	4.62	4.86	-0.24	6.35	-1.87	36
(<i>RR</i>)-Methylphenidate*	43.8	4.36	3.37	0.99	4.32	-0.503	33
Aniracetam amide	85.0	4.07	4.04	0.03	3.01	-0.603	31
Aniracetam lactam	95.0	4.02	3.47	0.55	4.51	-0.603	31
4-Nitrophenyl butyrate	130	3.89	4.56	-0.67	4.14	-1.18	30
Dilazep*	154	3.81	4.37	-0.56	4.45	-1.14	31
Imidapril*	287	3.54	4.12	-0.58	4.05	-0.892	31
5'-Phe-Floxuridine	460	3.34	3.33	0.01	4.51	-0.521	30
Benzapril*	734	3.13	3.37	-0.24	4.24	-0.483	31
4-Methylumbelliferyl acetate	800	3.10	2.51	0.59	6.48	-0.481	29
Cilazapril*	129	2.89	3.68	-0.79	5.62	-0.990	31
Irinotecan*	145	2.84	3.01	-0.17	5.65	-0.590	31
Delapril*	1500	2.82	3.09	-0.27	4.70	-0.422	31
Meperidine*	1900	2.72	3.26	-0.54	4.52	-0.481	29
5'-Asp-Floxuridine	3000	2.52	1.87	0.65	5.22	0.195	30
5'-Val-Floxuridine	3580	2.45	1.90	0.55	5.21	0.180	30
Heroin*	6300	2.20	2.87	-0.67	4.26	-0.188	32
6-Acetylmorphine*	8300	2.08	2.54	-0.46	4.37	-0.0103	32

The asterisk indicates the basic compounds; these were docked in both their protonated and neutral form. The data listed here refer to the neutral species.

Table 2B
Substrates included in the external test set

Substrate	Exp K_m (μM)	Exp pK_m	Pred pK_m	$\Delta(\text{exp} - \text{pred})$	Distance Ser221 (\AA)	MLP_{Ins}	Ref.
A8	1.50	5.82	5.47	0.35	4.74	-1.87	29
($\alpha R,1S$)- <i>trans</i> -A3	1.90	5.72	5.46	0.26	4.54	-1.81	29
trans-Resmethylrin	6.72	5.17	5.55	-0.37	4.75	-1.91	36
(<i>SR</i>)- <i>cis</i> -Permethrin	9.80	5.01	5.19	-0.18	5.89	-1.96	36
(<i>SS</i>)- <i>trans</i> -Permethrin	23.8	4.62	5.08	-0.46	5.91	-1.90	36
Clopidogrel*	55.7	4.25	5.14	-0.88	4.22	-1.54	34
(<i>SS</i>)-Methyl-phenidate*	89.9	4.05	3.88	0.17	4.85	-0.93	33
Cocaine*	120	3.92	3.82	0.10	3.40	-0.561	32
Quinapril*	134	3.87	4.46	-0.59	4.20	-1.13	31
Oseltamivir*	177	3.75	2.49	1.27	3.23	0.283	35
4-Nitrophenyl acetate	359	3.44	3.63	-0.19	4.08	-0.605	30
Camostat*	707	3.15	2.21	0.94	6.55	-0.316	31
Temocapril*	786	3.10	2.91	0.19	3.88	-0.125	31
5'-Leu-Floxuridine	970	3.01	2.31	0.70	4.60	0.0743	30
Capecitabine	1300	2.89	3.56	-0.68	3.97	-0.536	37

The asterisk indicates the basic compounds.

Table 3

Best three-variable correlations as derived from four series of docking experiments

Eq.	CES1	Ionization ^a	Equation ^{b,c,d,e}	Statistics
1	Apo	N	$pK_m = -1.26(\pm 0.16) \text{MLP}_{\text{Ins}}$ -0.168(± 0.096) $\text{Dist}_{\text{Ser}221}$ $-2.54 \times 10^{-3}(\pm 7.83 \times 10^{-4})$ Volume +4.35(± 0.51)	$n = 25$; $r^2 = 0.87$; $s = 0.38$; $F = 44.96$
2	Apo	N+	$pK_m = -0.470(\pm 0.012) \text{MLP}_{\text{Ins}}$ $8.13 \times 10^{-3}(\pm 1.6 \times 10^{-4})$ PSA $5.21 \times 10^{-3}(\pm 1.6 \times 10^{-4})$ Zapbind +4.47(± 0.24)	$n = 25$; $r^2 = 0.75$; $s = 0.46$; $F = 16.83$
3	Holo	N	$pK_m = -1.07(\pm 0.15) \text{MLP}_{\text{Ins}}$ 0.111(± 0.073) $\text{Dist}_{\text{Ser}221}$ $-3.60 \times 10^{-3}(\pm 6.7 \times 10^{-4})$ Volume +4.45(± 0.45)	$n = 25$; $r^2 = 0.71$; $s = 0.50$; $F = 14.26$
4	Holo	N+	$pK_m = -0.697(\pm 0.130) \text{MLP}_{\text{Ins}}$ $8.75 \times 10^{-3}(\pm 2.0 \times 10^{-4})$ PSA $8.69 \times 10^{-3}(\pm 2.1 \times 10^{-4})$ Zapbind +4.02(± 0.25)	$n = 25$; $r^2 = 0.66$; $s = 0.56$; $F = 13.01$

^a Ionization state of basic substrates: N = neutral forms; N+ = protonated forms.^b MLP_{Ins} = Molecular Lipophilicity Potential (MLP) Interaction Score.^c Dist_{Ser221} = distance between the carbon atom of substrate's ester group and the hydroxy function of Ser221.^d PSA = polar surface area.^e Zapbind = Zapbind score, which accounts for electrostatic interactions based on a combination of surface contact terms and Poisson–Boltzman energy approximations (as computed by the ZAP module).

algorithm²⁵ ($r^2 = 0.48$), the substitution of log P in lieu of MLP_{Ins} in Eqs. 1–4 (Table 3) markedly worsened their statistical parameters (e.g., r^2 decreases from 0.87 to 0.40 in Eq. 1). This emphasizes that MLP_{Ins} scores account for the mutual hydrophobic contacts between substrate and enzyme, an information not encoded in log P values, and one that plays a pivotal role in the equations reported.

The parameters included in the equations of the protonated substrates (Eqs. 2 and 4, Table 3) suggest that polar contacts play a significant role as indicated by the Zapbind score which accounts for electrostatic interactions based on a combination of surface contact terms and Poisson–Boltzman energy approximations (as computed by the ZAP module).²⁶ The role of polar contacts in these equations is also reflected in the ligand-based descriptor, that is, molecular volume for unprotonated substrates (Eqs. 1 and 3, Table 3) and polar surface area (PSA) for the protonated ones (Eqs. 2 and 4, Table 3). The prevailing role of ionic contacts may also justify the modest statistics derived for ionized substrates whose binding mode is largely affected by electrostatic contacts and no longer reflects the different reactivity of the docked substrates.

Finally, it is interesting to observe that the correlations for the compounds with unprotonated basic groups include the distance between the carbon atom of substrate ester group and the hydroxy function of Ser221 (Dist_{Ser221}). This distance codes for the ability of a molecule to assume a binding mode conducive to catalysis and is well understandable considering that docking calculations can simulate only the recognition phase between enzyme and substrates to the exclusion of the catalytic phase. In other words, a given compound can be found to elicit good binding interactions and high docking scores with an enzyme, yet fail to possess an appropriate target group or fail to allow its binding in a catalytically productive mode.

Taken globally, the reported correlations emphasize that apo_CES1 appears as the structure best suited to predict the hydrolysis of new esters, and that basic groups appear to interact preferentially in their unprotonated form. What is more, the best correlation described in Table 3 (Eq. 1), which includes three variables in analogy with the other equations, can be simplified to a two-variable correlation (Eq. 5) by discarding the molecular volume term, thus including only docking-based parameters. Eq. 5 proved successful as confirmed by statistical parameters and appears also more robust than Eq. 1 (Table 3) as suggested by the increased F value (64.06 vs 44.96). The normalized equation confirms

the reliability of such correlation revealing that the MLP_{Ins} score plays a clearly prevailing role related to Dist_{Ser221}.

$$\begin{aligned} pK_m &= -1.66(\pm 0.151) \text{MLP}_{\text{Ins}} - 0.381(\pm 0.112) \text{Dist}_{\text{Ser}221} \\ &\quad + 4.18(\pm 0.691) \\ [\text{p}K_m]_{\text{Norm}} &= -0.946 [\text{MLP}_{\text{Ins}}]_{\text{Norm}} - 0.296 [\text{dist}_{\text{Ser}221}]_{\text{Norm}} + 1.088 \\ n &= 25; r^2 = 0.85; r_{\text{cv}}^2 = 0.82; q^2 = 0.73; SE = 0.49; F = 64.06; \\ p &< 0.0001 \end{aligned} \quad (5)$$

With a view to further assess the predictive power of Eq. 5, an external test set of 15 new CES1 substrates was collected and their predicted pK_m values compared with the literature (Table 2B). Table 2B also shows the parameters obtained by docking experiments and used as values for the independent variables. The relation between experimental and predicted K_m values (Eq. 6) for this external test set affords an encouraging validation for the predictive power of Eq. 5. Eq. 6 is indeed a satisfactory one given its statistics, its slope being close to 45° ($\alpha = 47.5^\circ$):

$$\begin{aligned} \text{p}K_m(\text{pred}) &= 1.090 \text{ p}K_m(\text{exp}) - 0.411 \\ n &= 15; r^2 = 0.75; SE = 0.50; F = 39.40; p < 0.0001 \end{aligned} \quad (6)$$

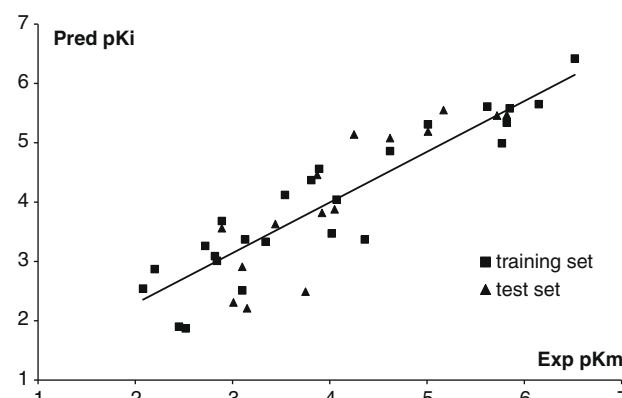


Figure 1. Correlation between experimental and predicted pK_m values. The plot emphasizes that there are not significant differences between the prediction of training set (■) and test set (▲).

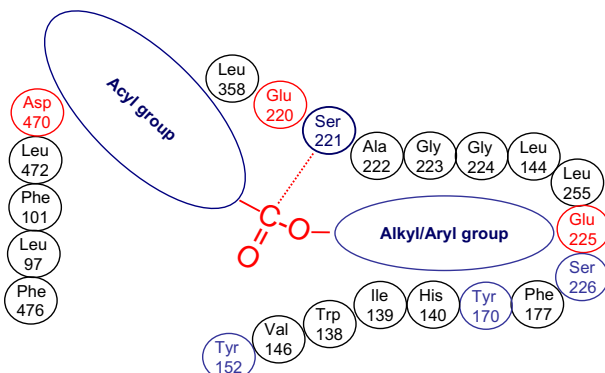


Figure 2. Two-dimensional scheme illustrating the main residues lining the catalytic pocket. The following color legend was used: polar residues = black; H-bonding residues = blue (including the catalytic residue Ser221); negatively charged residues = red.

Figure 1 confirms the predictivity of Eq. 5, showing that there are not clear differences between training and test sets. A more in-depth analysis of the predicted pK_m values reveals that for only one substrate in the test set the difference between experimental and predicted pK_m values is greater than 1 (oseltamivir, $\Delta pK_m = 1.27$), whereas for nine substrates out of 15 the difference is below 0.5. The analysis of all residuals (training and test sets) shows that there is no correlation with the pK_m values suggesting that Eq. 4 is equally predictive for good and poor hCES1 substrates (plot not shown).

2.3. Docking results: the CES1 catalytic cavity

Figure 2 reports the main residues lining the hCES1 cavity showing that it is entirely surrounded by hydrophobic residues with a significant abundance of alkyl side-chains. The negatively charged residues in the catalytic cavity have the plausible role of

favoring the egress of enzymatic products and can also explain why the binding modes of the substrates with protonated basic groups are greatly influenced by ionic contacts as discussed above.

A more careful analysis of the *apo_CES1* catalytic cavity reveals that the Ser221 residue, which belongs to the catalytic triad and contacts the substrate, subdivides the cavity in two regions of quite different polarity. As depicted in Figure 2, the pocket that accommodates the substrate's alkyl/aryl moiety is narrower and lined by some polar residues including both negatively charged and hydrogen-bonding ones (e.g., Tyr170, Gln194, Glu225, Ser226, and Thr321). Conversely, the region that harbors the acyl portion is wider and lined by apolar residues (e.g., Leu97, Phe101, Val146, Ala148, Tyr152, Leu358, Leu363, and Leu472). The polar residues and its smaller size render the pocket accommodating the alkyl/aryl moiety more rigid than the acyl-binding region where aliphatic residues permit a considerable flexibility. These observations may explain why hCES1 prefers substrates with less bulky alkyl/aryl moieties and bulkier acyl moieties, and they also suggest that an optimal feature of hCES1 recognition should be an alkyl/aryl moiety relatively more polar than the acyl moiety and allowing interactions with the polar residues.

This suggestion is confirmed by Table 4 which compiles the fragmental log P and volume of the alkyl/aryl and acyl moieties of a dataset of 25 structurally diverse substrates taken from the 40 ligands investigated here (Table 2A and B). It appears that, on average, the alkyl/aryl moiety is less lipophilic than the acyl group (fragmental lipophilicity 1.55 ± 1.60 vs 2.12 ± 1.15), as verified in 19 out of the 25 substrates. Similarly, the acyl group is bulkier than the alkyl/aryl moiety ($175 \pm 111 \text{ \AA}^3$ vs $131 \pm 95 \text{ \AA}^3$), as also verified in 14 substrates out of 25, even if crystallographic studies²⁴ have shown that substrates with a very large alkyl/aryl groups can assume rotated poses in which the acyl moiety is harbored within the smaller and more polar subpocket. Such reversed binding modes can well explain the broad specificity of hCES1, and the sole esters that cannot be hydrolyzed by hCES1 are probably molecules with very large acyl and alkyl/aryl groups. The data compiled in Table 4 led to a fair relationship (Eq. 7) which, even if far from having

Table 4
Set of structurally diverse substrates used in the physicochemical profiling

Substrate	Exp K_m (μM)	Fragmental log P of acyl moiety	Fragmental log P of alkyl/aryl moiety	Fragmental volume (\AA^3) of acyl moiety	Fragmental volume (\AA^3) of alkyl/aryl moiety
(α , β -1R)- <i>cis</i> -A3	0.30	3.29	2.77	142.6	188.8
A8	1.50	3.25	2.77	118.9	188.8
<i>trans</i> -Resmethrin	6.72	2.66	4.47	149.6	168.5
(<i>S</i> , <i>R</i>)- <i>cis</i> -Permethrin	9.80	3.29	4.73	142.6	180.0
(<i>R</i> , <i>R</i>)-Methylphenidate	43.80	2.26	1.09	181.7	28.9
Clopidogrel	55.70	4.36	1.09	228.0	28.9
Aniracetam	85	1.31	-0.11	79.3	109.2
Cocaine	120	2.15	1.09	236.7	28.9
Quinapril	134	3.02	1.73	346.9	45.2
Oseltamivir	177	1.01	1.73	250.5	45.2
4-Nitrophenyl butyrate	130	2.82	2.85	77.6	104.4
Dilazep	154	2.33	3.54	160.2	386.3
Imidapril	287	2.56	1.73	311.5	45.2
4-Nitrophenyl acetate	359	1.09	2.85	28.9	106.8
5'-Phe-Floxuridine	460	2.12	-1.25	127.0	185.5
Benazepril	734	2.59	1.73	326.3	45.2
4-Methylumbelliferyl acetate	800	1.09	-0.62	28.9	144.6
Cilazapril	1295	3.05	1.73	333.5	45.2
Irinotecan	1453	0.97	1.81	334.3	189.0
Delapril	1502	3.43	1.73	364.0	45.2
Meperidine	1900	2.11	1.73	185.3	45.2
5'-Asp-Floxuridine	3000	-0.84	-1.25	79.7	185.5
5'-Val-Floxuridine	3580	1.47	-1.25	90.0	185.5
Heroin	6300	0.82	1.09	28.9	297.1
Monoacetylmorphine	8300	0.71	1.09	28.9	258.2
Mean \pm SD	—	2.12 \pm 1.15	1.55 \pm 1.60	175.3 \pm 111.5	131.3 \pm 95.0

a predictive power, seems to confirm the specific role of lipophilicity and steric hindrance in hCES1 substrates:

$$\begin{aligned} pK_m = & 0.474(\pm 0.16) \log P_{\text{acyl}} + 0.278(\pm 0.11) \log P_{\text{alkyl/aryl}} \\ & - 4.72 \times 10^{-3}(\pm 1.42 \times 10^{-3}) \text{Vol}_{\text{acyl}} + 3.18(\pm 0.37) \quad (7) \\ n = 25; r^2 = & 0.61; s = 0.75; F = 11.15; p < 0.0001 \end{aligned}$$

Eq. 7 emphasizes the relevance of lipophilicity for both moieties even if the coefficients of the two $\log P$ descriptors indicate that the lipophilicity of the acyl group plays a more relevant role. Eq. 7 also confirms the relevance of molecular volume even if it only includes the volume of the acyl moiety.

The described correlations and the above considerations on the hCES1 cavity shed light on some key features common to all complexes examined. First, the ester group in the ligands must come close to the hydroxy function of Ser221. This mandatory contact was used to select the best binding modes for each substrate and

appears in Eqs. 1–4 (Table 3) as a key descriptor to predict hCES1 activity. Second, the soundness of docking results was also verified by checking the distance between the carbonyl oxygen atom of the substrates and the ‘oxyanion hole’ as defined by the backbone atoms of Gly142 and Gly143, another interaction playing a critical role in the catalytic mechanism.

Furthermore, the analysis of the hCES1 cavity underlines the key role of hydrophobic interactions especially with the acyl moiety of substrates. The relevance of such contacts is also confirmed by the MLP_{Ins} scores which appear in all correlations. The different distribution of aliphatic and aromatic residues in the two subcavities also suggests that aromatic rings are accommodated better when they are part of the alkyl/aryl moiety, where they can interact with some aromatic residues (His140, Tyr152, Tyr170, and Tyr177).

As mentioned, the negatively charged residues in the hCES1 cavity can explain the preference of the enzyme for neutral sub-

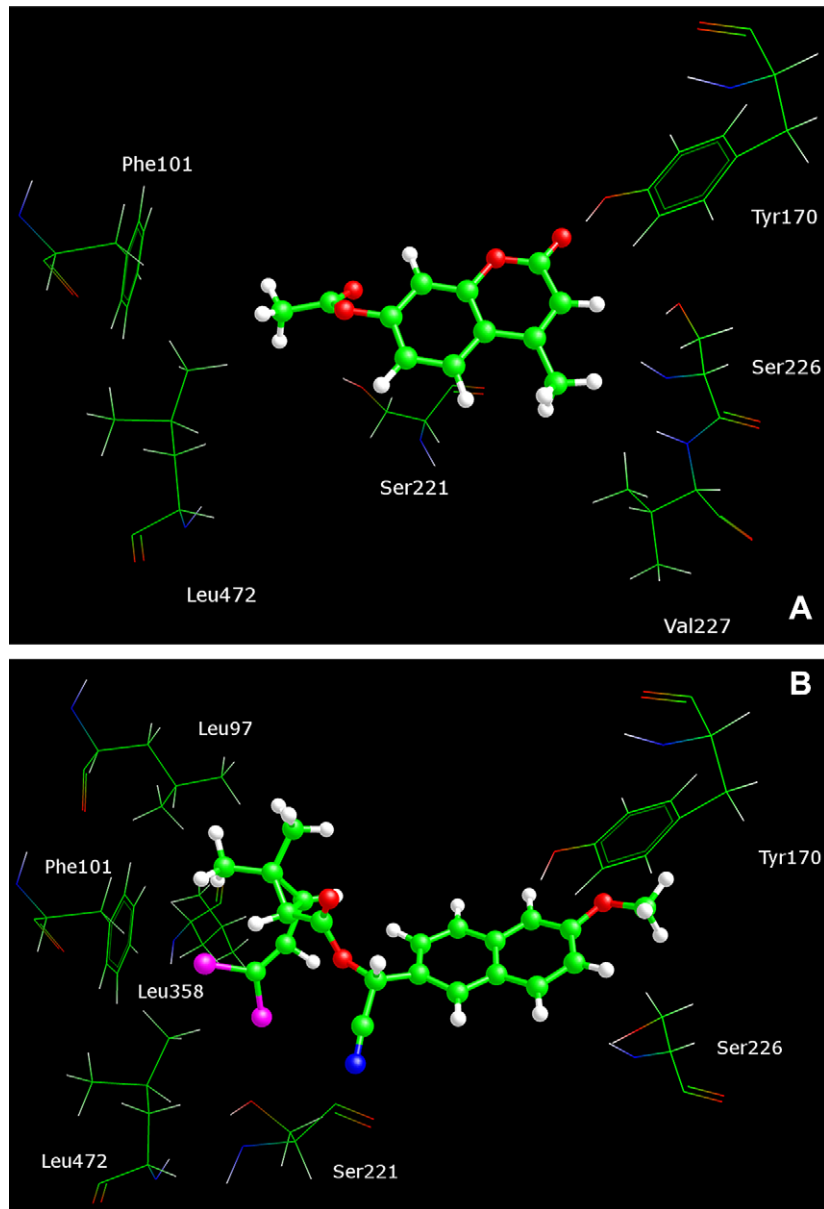


Figure 3. Main interactions stabilizing the putative complex of hCES1 with 4-methylumbelliferyl acetate (A) and the pyrethroid ($\alpha R,1R$)-cis-A3 (B). One can note in both complexes the catalytic interaction with Ser221 as well as the H-bond between the aryl substituents and Ser226 and Tyr170, while the acyl groups mainly elicit apolar contacts.

strates and, more generally, suggest that cationic ligands which interact too strongly by ionic bonds cannot be good CES1 substrates because they are trapped in the cavity in unproductive modes and behave as inhibitors. This observation is in line with the known promiscuity of the enzyme, which is known to interact with structurally diverse substrates, a fact consistent with the present rationalization that a variety of hydrophobic interactions plus some weak polar interactions are enough to make a compound behave as a good hCES1 substrate.

2.4. Docking results: analysis of the putative complexes

The above considerations find compelling evidence when analyzing the putative enzyme–substrate complexes. Thus, 4-methylumbelliferyl acetate (Fig. 3A) accommodates the ester function with the carbon atom of the carbonyl group reasonably close to Ser221, while the oxygen atom of carbonyl group interacts conveniently with Gly142 and Gly143 in the oxyanion hole. Furthermore, the oxochromonyl moiety stabilizes H-bonds with Tyr170, a polar contact shared by many computed complexes, and the aryl moiety generates π – π interactions with aromatic residues (e.g., His140, Tyr152, and Tyr170), thus reinforcing the stability of the complex.

The aryl moiety of this substrate realizes a rich pattern of interactions with the enzyme, while its low affinity (high K_m value) can be ascribed to the small size of its acyl moiety which confers hCES2 selectivity. Similarly, 4-nitrophenyl acetate and 4-nitrophenyl butyrate bind in the enzyme so that their ester moiety contacts Ser221 and the oxyanion hole, while the nitro group realizes an H-bond with Tyr170. Again, the high K_m values of these substrates are understandable considering their small acyl portion.

The pyrethroids, as exemplified in Figure 3B by the complex with ($\alpha R, 1R$)-*cis*-A3, emphasize the relevant role of apolar contacts produced by the acyl group. Indeed, their hydrophobic chrysanthemoyl moiety can interact with several aliphatic residues (e.g., Leu97, Val146, Leu363, Leu358, and Leu472), while the H-bonding groups in the alkyl/aryl moiety elicit the known interaction with Tyr170. Such a rich interaction pattern is shared by almost all pyrethroids considered and explains the marked efficacy with which hCES1 hydrolyzes such esters. The stereoselective hydrolysis of methylphenidate is well explained considering that only the (*R,R*)-stereoisomer accommodates the phenyl ring close to many apolar residues (e.g., Val254, Leu255, Leu358, Leu359, Leu363, Met425, and Phe426), while the piperidine ring stabilizes H-bond with Glu220.³³

The analysis of the computed complexes for the six angiotensin-converting enzyme (ACE) inhibitors underlines the critical role of apolar contacts formed by the acyl moiety in the catalytic pocket. In particular, the acyl portion assumes therein a folded conformation which allows several hydrophobic interactions, while the polar groups do not realize specific polar contacts. Despite their zwitterionic character, these ACE inhibitors seem to confirm the detrimental role of positive charges on hCES1 catalysis. Indeed, the presence of a basic group can explain why such substrates have, on average, quite high K_m values despite the many hydrophobic contacts they can create.

Given the significant size and rigidity of its aryl moiety, irinotecan is a relevant example of a substrate which assumes a rotated binding mode. Thus, its lactam ring forms a H-bond with Thr298 and its 4-hydroxy group interacts with Asp90, while the apolar skeleton of the fused pentacyclic system elicits hydrophobic interactions with the apolar/aromatic residues mentioned above. Finally, the complexes for the nucleoside analogues are in line with the literature.³⁰ Thus, the uracil ring in 5'-Phe-uridine forms H-bonds with Tyr170 and His140, while the aminoacyl promoiety contacts Tyr152 plus several alkyl side-chains.

2.5. MD simulations

Molecular dynamics simulations were carried out on hCES1 complexed with the substrates and products involved in heroin hydrolysis, our objective being to investigate the stability of the computed complexes, the pathways of product egress, and the influence of protonation on the *in situ* behavior of ligands. As schematized in the inset of Figure 4, heroin is hydrolyzed by two hCES1-catalyzed reactions, first to 6-O-acetylmorphine and then to morphine. As reported in Table 2A, heroin and 6-O-acetylmorphine are very poor substrates for hCES1 ($K_m = 6300$ and $8300 \mu\text{M}$, respectively) and indeed these hydrolytic reactions are also catalyzed by hCES2 and serum butyrylcholinesterase (hBuChE).

The hydrolysis of heroin was selected for two reasons, (a) because heroin and 6-acetylmorphine are the poorest substrates among the molecules investigated here and therefore offer the most stringent conditions to assess the stability of complexes with hCES1; and (b) because their basicity and poor affinity again afford good conditions to examine whether the latter behavior (poor affinity) is due to the former property (basicity). In fact, the poor activity of hCES1 toward heroin and its metabolite can also be explained by the fact that these substrates have a higher affinity for hCES2 than for hCES1, having a large alkyl/aryl moiety and a small acyl moiety. Nevertheless, one can postulate that their basic alkyl/aryl moiety can hamper catalytic efficiency since protonated forms may elicit strong electrostatic interactions within the enzymatic cavity thus blocking catalytic turnover.

Six MD runs were carried out to simulate hCES1 complexed with heroin, 6-acetylmorphine and morphine in both neutral and protonated form. The resulting trajectories were analyzed by monitoring how the distance between Ser221 and the target ester group in heroin and 6-acetylmorphine varied during the duration of the simulations (5 ns). A preliminary analysis had examined the protein stability as assessed by the percentage of residues which remained in the allowed regions of the Ramachandran plot. It was found that the simulations did not undermine the folding stability of the protein since the percentage remained constantly around 75% during all MD runs. Globally, such a result suggests that the differences in behavior described below are mainly due to the dynamic response of the enzyme and bound ligands and not to random structural distortions.

Figure 4 shows the distance profile of the two electrical forms of heroin. Clearly the ligand remained close to the catalytic site over

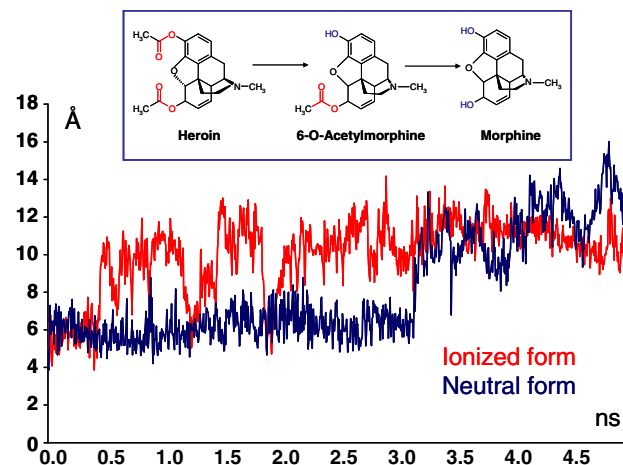


Figure 4. The dynamic profile for the distance between Ser221 and the 3-ester group of heroin as obtained in 5 ns MD simulations (blue line = neutral heroin; red line = protonated heroin). The inset schematizes the hydrolysis of heroin as catalyzed by hCES1.

the entire simulation time irrespective of the electrical state of the ligand. This result confirms the stability of the computed complexes and suggests that the behavior of this substrate is not markedly influenced by its ionization state. The variability in the monitored distance as seen in Figure 4 was mainly due to the presence of the two hydrolyzable groups in heroin so that Ser221 can bounce between them. There is however a significant difference between the two MD simulations since the 3-ester group remained markedly closer to Ser221 than the 6-ester group (5.23 vs 9.44 Å) in neutral heroin, while the ionized substrate maintained its two ester groups at similar average distances with Ser221 (9.96 vs 10.13 Å). This result suggests that the simulation with neutral heroin can account for the regioselectivity of the hCES1-catalyzed hydrolysis toward the 3-ester group, whereas the MD run with ionized heroin is so affected by ionic interactions that these cancel the difference in reactivity of the two ester groups.

6-Acetylmorphine, the second substrate examined (Fig. 5), also remained close to the catalytic site during the simulation time, irrespective of its electrical state. The two distance profiles were quite similar probably due to the presence of a single target group. Taken together, the simulations with heroin and 3-acetylmorphine confirm the stability of the computed complexes and indicate that the substrate behavior shows moderate dependence on its ionization state, although the neutral forms seem to yield more realistic simulations in which the key contacts with the enzyme are not biased by ionic interactions.

In MD simulations involving morphine as a product, we monitored the distance between its 3-aryl moiety and Ser221. Here, a totally different result was seen depending on the ionization state of the metabolite. Indeed, its protonated form remained anchored to the catalytic site during the entire simulation period (Fig. 6), whereas neutral morphine moved away rapidly from Ser221 and made a progressive exit from the enzymatic cavity. These MD runs clearly indicate that a protonated ligand can remain trapped in the catalytic site and behaves as an inhibitor when it forms ionic bonds with some acidic residue(s).

Globally, the simulations afford evidence that hCES1 preferentially recognizes basic substrates in their neutral form. Indeed, (a) docking results reveal that the binding modes and binding stability of ligands with positively charged groups are markedly affected by electrostatic interactions, so much so that they do not reflect the differences in reactivity of the substrates, as evidenced by poor correlations for protonated substrates; and (b) MD simulations show that the protonated products cannot leave the catalytic cavity and must behave as inhibitors. One can assume such an entrapment to be particularly strong when the basic group is borne

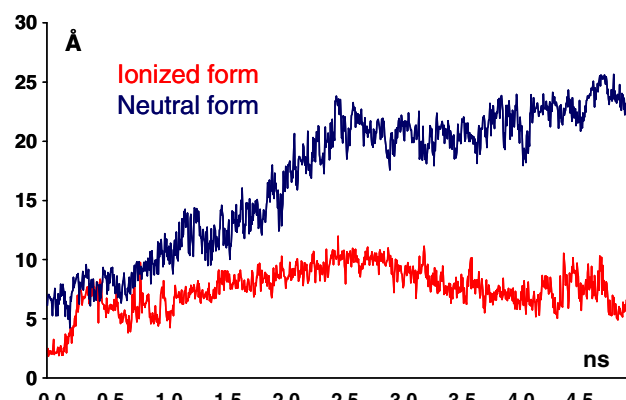


Figure 6. The dynamic profile for the distance between Ser221 and the 3-aryl moiety of morphine as obtained in 5 ns MD simulations (blue line = neutral morphine; red line = protonated morphine).

by the alkyl/aryl moiety as in morphine, whereas the effects of a positive charge in the acyl moiety can be partially counteracted by the free carboxylate function liberated by the hydrolytic reaction.

Conversely, the MD simulation for neutral morphine shows that the enzymatic product can freely move away from the catalytic site allowing an efficient catalytic turnover. This result has a double relevance. First, it confirms that MD simulations are able to successfully discriminate between substrates and products even when the structural difference between them is modest. More generally, one can argue that such simulations are also able to discriminate between substrates (which remain near Ser221) and non-substrates (which promptly leave the catalytic cavity), providing a useful even if time-demanding tool to investigate at atomic level the metabolic fate of new medicinal esters.

Second, the simulation with neutral morphine affords a clear picture of the pathway covered by the metabolite during its exit. From a methodological standpoint this result confirms that the product egress can be simulated by standard all-atom-MD simulations without artifacts or constraints, whereas most analyses of product exit hitherto published involved targeted simulations in which the egress was induced by applying external forces.²⁷ Moreover, this MD run allows the recognition of hCES1 residues which facilitate product exit, unveiling that the product pathway is largely surrounded by apolar residues (Val254, Leu358, Met364, Pro387, and Cys390); only when the product reaches the hCES1 surface does it approach some polar residues (Ser253, Lys257, and Lys302).

3. Conclusions

The simulations described here suggest that a reasonable prediction of the hydrolytic metabolism of hCES1 substrates is possible. On the one hand, this study fills a gap because the hydrolytic activity of human esterases was never investigated by *in silico* approaches. On the other hand, this is the first step in an attempt to predict the hydrolytic stability of new chemical entities; other relevant human esterases such as hCES2 and hBuChE should be analyzed by similar computational methodologies in order to attain a broader prediction of the hydrolytic metabolism for a given medicinal ester.

Encouragingly, the MLP_{Ins} score used here appears useful in docking analyses to parameterize the often disregarded hydrophobic interactions even if the relevance of such a score is also based on its capacity to account for some polar interactions such as H-bonds. Again, the MLP_{Ins} score fills a gap since specific score

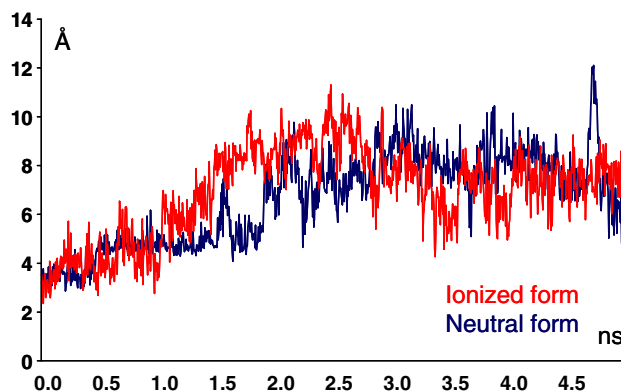


Figure 5. The dynamic profile for the distance between Ser221 and the ester group of 6-O-acetylmorphine as obtained in 5 ns MD simulations (blue line = neutral 6-O-acetylmorphine; red line = protonated 6-O-acetylmorphine).

functions for apolar contacts are rarely reported although the importance of hydrophobic contacts in protein recognition is widely recognized.²⁸ Clearly, the MLP_{INS} score, which now is implemented in VEGA software (www.vegazz.net), should be tested in many other docking studies to verify its potential; only then could it be embedded in a docking program to guide the search engine of docking modes without limiting its use to the sole scoring of final complexes.

4. Computational details

4.1. Preparation of CES1 structures

Nine X-ray structures of the human CES1 (as detailed in Section 3 and compiled in Table 1) were retrieved from the Protein Database. Irrespective of the number of monomers included in the crystal structure, the calculations involved always a single monomer, since it is catalytically self-sufficient. The nine monomers were completed by adding hydrogen atoms, and the side-chains of Arg, Lys, Glu, and Asp were ionized to remain compatible with physiological pH values, while His residues were considered neutral by default. The structures so obtained were minimized, keeping the backbone fixed to preserve the experimental folding, and evaluated by the pair-wise matching as compiled in Table 1.

The experimental structure of hCES1 complexing naloxone methiodide was used in the docking simulations without other significant refinements; in contrast, its resolved structure when complexed with the inhibitor benzil was slightly modified since the catalytic site was too narrow to accommodate large substrates. Hence the binding site was gradually enlarged by docking a small set of three known substrates of increasing volume (i.e., 4-methylumbelliferyl acetate, ($\alpha R; 1R$)-*cis*-A3, and quinapril). Each ligand was docked manually into the hCES1 catalytic site so that the ester group was reasonably close to Ser221, and each complex was then minimized keeping fixed all atoms beyond a 15 Å radius sphere around the bound substrate in order to expand the catalytic site without distorting protein folding. After a final minimization with the backbone fixed, the hCES1 structure underwent docking simulations as described below. It should be noted that the manual

docking was exploited only to enlarge the catalytic site; all complexes described in Section 3 and used to develop correlative equations were obtained by automatic docking simulations as detailed later.

4.2. Ligand dataset

A ligand dataset of 40 known CES1 substrates was collected from the literature by selecting molecules whose CES-catalyzed hydrolysis was determined using purified recombinant hCES1 and expressed as K_m (μM, as compiled in Table 2A and B and Figure 7).^{29–37} The ionizable substrates were docked considering the most probable form at physiological pH, although all simulations were repeated with the basic groups in their unprotonated state. The conformational behavior of the compounds was investigated by a MonteCarlo procedure (as implemented in the VEGA suite of programs³⁸) which generated 1000 conformers by randomly rotating the rotors. All geometries so obtained were stored and optimized to avoid high-energy rotamers. The 1000 conformers were clustered according to their similarity to discard redundant ones; in this analysis two geometries were considered as non-redundant when they differed by more than 60° in at least one torsion angle. As described under Section 3, the ligand dataset was subdivided in the training ($n = 25$) and test ($n = 15$) sets. Even if randomly subdivided, the Tanimoto comparison of the chemical fingerprints for substrates included in the two sets indicates that they have a similar average variability (0.26 vs 0.28)³⁹ suggesting that they cover equally the chemical space of CES1 substrates.

4.3. Docking analyses and definition of MLP interaction score

The docking and scoring procedure involved extensive rigid-body sampling with the OpenEye Scientific Software package FRED. Sampling was performed in a cube of 10 Å sides around Ser221, which is the critical catalytic residue. The best complexes were minimized keeping fixed all atoms outside a 15 Å radius sphere around the bound substrate to favor the mutual adaptability between ligand and enzyme. The optimized complexes were then used to calculate FRED's docking scores and the Molecular Lipo-

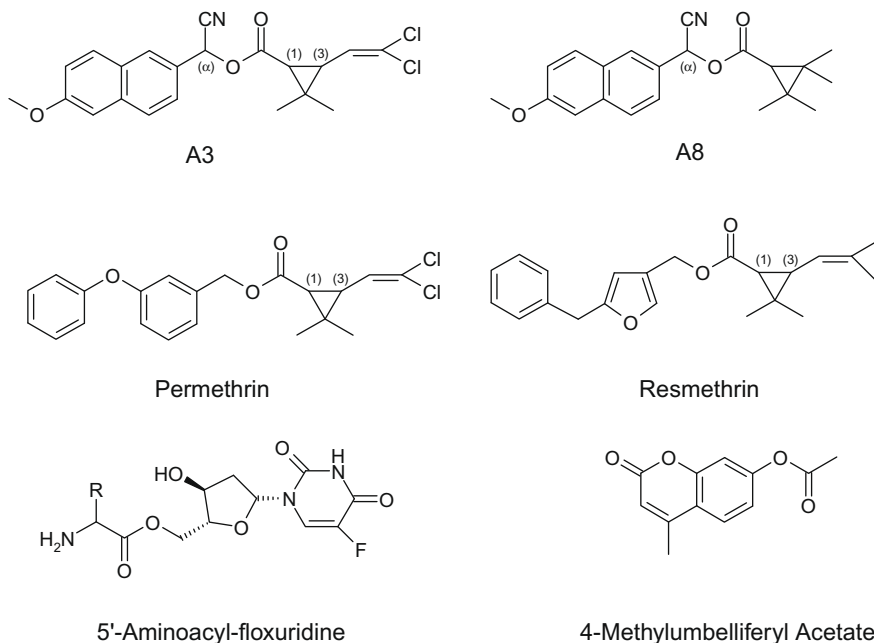


Figure 7. Chemical structure of the lesser known substrates investigated in this study.

philicity Potential (MLP) Interaction Score (MLP_{Ins} , see below). In the statistical analyses (Table 2A and B), a small set of representative physicochemical properties of the bound ligands (e.g., virtual log P , PSA, SAS, volume, and dipole moment) were also taken into account.

The MLP Interaction Score (MLP_{Ins}) was computed using the atomic fragmental system proposed by Broto et al.⁴⁰ and a distance function that defined how the score decreased with increasing distance between interacting atoms. In detail, the equation to compute such an interaction score is reported below (Eq. 8), where f_a and f_b denote the lipophilicity increments for a pair of atoms and r_{ab} is the distance between them. The first sum (p) concerns all ligand's atoms and the second (m) all enzyme's atoms.

The basic assumption in the calculation of the MLP_{Ins} , which encodes the contributions of the various intermolecular forces

$$\text{MLP}_{\text{Ins}} = \sum_p \sum_m -\frac{(f_a \cdot f_b)}{f(r_{ab})} \quad (8)$$

measured experimentally in partition coefficients, is that the score is favorable (i.e., negative) when both increments have the same sign (as denoted by the negative sign in Eq. 8), or unfavorable (repulsive forces) when the score has a positive sign. When the atomic parameters are both positive, MLP_{Ins} encodes hydrophobic interactions and dispersion forces, the importance of which is well recognized in docking simulations, and it accounts for polar interactions, in particular H-bonds and electrostatic forces when the atomic parameters are both negative.⁴¹ Several distance functions (e.g., linear, quadratic, cubic, and Fermi's type) were tested, checking also dual functions depending on the signs of the atomic increments (e.g., linear function when f_a and f_b are both negative and r^6 for hydrophobic and repulsive interactions). Such dual functions come from the consideration that polar contacts are long-range interactions, while dispersion and hydrophobic contacts are very short-range ones.⁴² Nonetheless, a cubic distance function was finally selected, since MLP_{Ins} scores with dual functions tend inevitably to undervalue the contribution of the apolar contacts, becoming a descriptor of ionic interactions, while a cubic function should represent a proper balance between short- and long-range interactions.

4.4. MD simulations

MD simulations involving hCES1 in complex with heroin, 6-acetylmorphine and morphine were performed, with the ligands both in their neutral and protonated forms. The complexes of hCES1 with heroin and 6-acetylmorphine were taken from docking results, while the complex of the enzyme with morphine was generated by manually transforming the enzyme complexed with 6-acetylmorphine. The complex with morphine was then minimized keeping fixed all atoms outside a 15 Å radius sphere around the bound product before performing the MD simulation.

The complexes so obtained were inserted into a 50 Å radius sphere of water molecules, and, after a preliminary minimization to optimize the relative position of solvent molecules, the systems underwent 5 ns of all-atoms MD simulations with the following characteristics: (a) spherical boundary conditions were introduced to stabilize the simulation space; (b) Newton's equation was integrated using the r-RESPA method (every 4 fs for long-range electrostatic forces, 2 fs for short-range non-bonded forces, and 1 fs for bonded forces); (c) the temperature was maintained 300 ± 10 K by means of Langevin's algorithm; (d) Lennard-Jones (L-J) interactions were calculated with a cut-off of 10 Å and the pair list was updated every 20 iterations; (e) a frame was stored every 5 ps, yielding 1000 frames; and (f) no constraints were applied to the systems.

The simulations were carried out in two phases: an initial period of heating from 0 to 300 K over 6000 iterations (6 ps, i.e., 1 K/20 iterations), and a monitored phase of simulation of 5 ns. Only the frames memorized during this last phase were considered. The calculations described here were carried out on a 16 CPU Tyan-VX50 system using Namd2.6⁴³ with the force field CHARMM and Gasteiger's atomic charges.

References and notes

- Vistoli, G.; Pedretti, A.; Testa, B. *Drug Discovery Today* **2008**, *13*, 285.
- Testa, B.; Krämer, S. D. *Chem. Biodiv.* **2006**, *3*, 1053.
- Czodrowski, P.; Kriegel, J. M.; Scheuerer, S.; Fox, T. *Expert Opin. Drug Metab. Toxicol.* **2009**, *5*, 15.
- Testa, B.; Krämer, S. D. *Chem. Biodiv.* **2007**, *4*, 257.
- Stjernschantz, E.; Vermeulen, N. P.; Oostenbrink, C. *Expert Opin. Drug Metab. Toxicol.* **2008**, *4*, 513.
- Edmondson, D. E.; Mattevi, A.; Binda, C.; Li, M.; Hubálek, F. *Curr. Med. Chem.* **2004**, *11*, 1983.
- Carballeira, J. D.; Quezada, M. A.; Alvarez, E.; Sinisterra, J. V. *Molecules* **2004**, *9*, 673.
- Testa, B.; Krämer, S. D. *Chem. Biodiv.* **2008**, *5*, 2171.
- Smith, P. A.; Sorich, M. J.; Low, L. S.; McKinnon, R. A.; Miners, J. O. *J. Mol. Graphics Modell.* **2004**, *22*, 507.
- Najmanovich, R. J.; Allali-Hassani, A.; Morris, R. J.; Dombrovsky, L.; Pan, P. W.; Vedadi, M.; Plotnikov, A. N.; Edwards, A.; Arrowsmith, C.; Thornton, J. M. *Bioinformatics* **2007**, *23*, 104.
- Sipilä, J.; Taskinen, J. *J. Chem. Inf. Comput. Sci.* **2004**, *44*, 97.
- Soffers, A. E.; Ploemen, J. H.; Moonen, M. J.; Wobbes, T.; van Ommen, B.; Vervoort, J.; van Bladeren, P. J.; Rietjens, I. M. *Chem. Res. Toxicol.* **1996**, *9*, 638.
- Testa, B.; Mayer, J. M. *Hydrolysis in Drug and Prodrug Metabolism—Chemistry, Biochemistry and Enzymology*; Wiley-VCH: Weinheim, Germany, 2003.
- Hatfield, J. M.; Wierdl, M.; Wadkins, R. M.; Potter, P. M. *Expert Opin. Drug Metab. Toxicol.* **2008**, *4*, 1153.
- Ettmayer, P.; Amidon, G. L.; Clement, B.; Testa, B. *J. Med. Chem.* **2004**, *47*, 2393.
- Testa, B. *Curr. Opin. Chem. Biol.* **2009**, *13*, 338.
- Imai, T. *Drug Metab. Pharmacokinet.* **2006**, *21*, 173.
- Hosokawa, M. *Molecules* **2008**, *13*, 412.
- Testa, B.; Krämer, S. D. *Chem. Biodiv.* **2007**, *4*, 2031.
- Satoh, T.; Hosokawa, M. *Annu. Rev. Pharmacol. Toxicol.* **1998**, *38*, 257.
- Satoh, T.; Hosokawa, M. *Chem. Biol. Interact.* **2006**, *162*, 195.
- Totrov, M.; Abagyan, R. *Curr. Opin. Struct. Biol.* **2008**, *18*, 178.
- Fleming, C. D.; Bencharit, S.; Edwards, C. C.; Hyatt, J. L.; Tsurkan, L.; Bai, F.; Fraga, C.; Morton, C. L.; Howard-Williams, E. L.; Potter, P. M.; Redinbo, M. R. *J. Mol. Biol.* **2005**, *352*, 165.
- Bencharit, S.; Morton, C. L.; Xue, Y.; Potter, P. M.; Redinbo, M. R. *Nat. Struct. Biol.* **2003**, *10*, 349.
- Gaillard, P.; Carrupt, P. A.; Testa, B.; Boudon. *J. Comput. Aided Mol. Des.* **1994**, *8*, 83.
- Prabhu, N. V.; Zhu, P.; Sharp, K. A. *J. Comput. Chem.* **2004**, *25*, 2049.
- Pedretti, A.; Bocci, E.; Maggi, R.; Vistoli, G. *Steroids* **2008**, *73*, 708.
- Pyrkov, T. V.; Chugunov, A. O.; Krylov, N. A.; Nolde, D. E.; Efremov, R. G. *Bioinformatics* **2009**, *25*, 1201.
- Nishi, K.; Huang, H.; Kamita, S. G.; Kim, I. H.; Morisseau, C.; Hammock, B. D. *Arch. Biochem. Biophys.* **2006**, *445*, 115.
- Ladowski, C. P.; Lorenzi, P. L.; Song, X.; Amidon, G. L. *J. Pharmacol. Exp. Ther.* **2006**, *316*, 572.
- Takai, S.; Matsuda, A.; Usami, Y.; Adachi, T.; Sugiyama, T.; Katagiri, Y.; Tatematsu, M.; Hirano, K. *Biol. Pharm. Bull.* **1997**, *20*, 869.
- Pindel, E. V.; Kedishvili, N. Y.; Abraham, T. L.; Brzezinski, M. R.; Zhang, J.; Dean, R. A.; Bosron, W. F. *J. Biol. Chem.* **1997**, *272*, 14769.
- Sun, Z.; Murry, D. J.; Sanghani, S. P.; Davis, W. I.; Kedishvili, N. Y.; Zou, Q.; Hurley, T. D.; Bosron, W. F. *J. Pharmacol. Exp. Ther.* **2004**, *310*, 469.
- Tang, M.; Mukundan, M.; Yang, J.; Charpentier, N.; LeCluyse, E. L.; Black, C.; Yang, D.; Shi, D.; Yan, B. *J. Pharmacol. Exp. Ther.* **2006**, *319*, 1467.
- Shi, D.; Yang, J.; Yang, D.; LeCluyse, E. L.; Black, C.; You, L.; Akhlaghi, F.; Yan, B. *J. Pharmacol. Exp. Ther.* **2006**, *319*, 1477.
- Ross, M. K.; Borazjani, A.; Edwards, C. C.; Potter, P. M. *Biochem. Pharmacol.* **2006**, *71*, 657.
- Quinney, S. K.; Sanghani, S. P.; Davis, W. I.; Hurley, T. D.; Sun, Z.; Murry, D. J.; Bosron, W. F. *J. Pharmacol. Exp. Ther.* **2005**, *313*, 1011.
- Pedretti, A.; Villa, L.; Vistoli, G. *J. Mol. Graphics Modell.* **2002**, *21*, 47.
- Gordon, J. W.; Xue, L.; Bajorath, J. *J. Chem. Inf. Comput. Sci.* **2000**, *40*, 163.
- Broto, P.; Moreau, G.; Vandycke, C. *Eur. J. Med. Chem.* **1984**, *19*, 66.
- Testa, B.; Carrupt, P. A.; Gaillard, P.; Billois, F.; Weber, P. *Pharm. Res.* **1996**, *13*, 335.
- Stone, A. J. *Science* **2008**, *321*, 787.
- Phillips, J. C.; Braun, R.; Wang, W.; Gumbart, J.; Tajkhorshid, E.; Villa, E.; Chipot, C.; Skeel, R. D.; Kalé, L.; Schulten, K. *J. Comput. Chem.* **2005**, *16*, 1781.